

## Accepted Manuscript

A near-infrared fluorescent probe for rapid detection of carbon monoxide in living cells

Liqiang Yan, Ding Nan, Cheng Lin, Yi Wan, Qiang Pan, Zhengjian Qi



PII: S1386-1425(18)30452-9  
DOI: doi:[10.1016/j.saa.2018.05.059](https://doi.org/10.1016/j.saa.2018.05.059)  
Reference: SAA 16093

To appear in: *Spectrochimica Acta Part A: Molecular and Biomolecular Spectroscopy*

Received date: 26 December 2017  
Revised date: 13 May 2018  
Accepted date: 15 May 2018

Please cite this article as: Liqiang Yan, Ding Nan, Cheng Lin, Yi Wan, Qiang Pan, Zhengjian Qi , A near-infrared fluorescent probe for rapid detection of carbon monoxide in living cells. The address for the corresponding author was captured as affiliation for all authors. Please check if appropriate. Saa(2017), doi:[10.1016/j.saa.2018.05.059](https://doi.org/10.1016/j.saa.2018.05.059)

This is a PDF file of an unedited manuscript that has been accepted for publication. As a service to our customers we are providing this early version of the manuscript. The manuscript will undergo copyediting, typesetting, and review of the resulting proof before it is published in its final form. Please note that during the production process errors may be discovered which could affect the content, and all legal disclaimers that apply to the journal pertain.

## A near-infrared fluorescent probe for rapid detection of Carbon Monoxide in living cells

Liqiang Yan<sup>a\*</sup>, Ding Nan<sup>b</sup>, Cheng Lin<sup>b</sup>, Yi Wan<sup>b</sup>, Qiang Pan<sup>b</sup>, Zhengjian Qi<sup>b\*</sup>

<sup>a</sup> College of Chemistry and Bioengineering, Guilin University of Technology, Guilin 541004, PR China

<sup>b</sup> College of Chemistry and Chemical Engineering, Southeast University, Nanjing, Jiangsu 211189, PR China

Corresponding author: liqiangyan@glut.edu.cn (Liqiang Yan); qizhengjian506@163.com (Zhengjian Qi)

### Abstract:

A near-infrared (NIR) and colorimetric fluorescent probe system was developed for Carbon Monoxide (CO) via a Pd<sup>0</sup>-mediated Tsuji-Trost reaction. In this probe, phenoxide anion formation (DPCO<sup>-</sup>) was acted as the signal unit and an allyl carbonate group was used as the recognition unit. This non-fluorescent probe molecule can release the relevant fluorophore after conversion of Pd<sup>2+</sup> to Pd<sup>0</sup> by CO. The probe system including probe 1 and Pd<sup>2+</sup> can be used for “naked-eye” detection of CO, and exhibited high selectivity to CO over various other sensing objects. More importantly, the probe system has great potential for fluorescence imaging of intracellular CO in living cells.

**Keywords:** Near-infrared, Fluorescence probe, Carbon Monoxide, Living cells

### 1. Introduction

In the human body and other biological systems, carbon monoxide (CO) can be endogenously produced during the haem catabolism by heme oxygenase (HO) enzymes, which is an important cell signaling molecule with substantial therapeutic potential protecting from vascular, inflammatory, or even cancer diseases. [1, 2] More importantly, it is now evident that CO can be used as a potential therapeutic agent because of its reported antihypertensive, anti-inflammatory and cell-protective effects. [3] Therefore, it is critically required to develop “smart” noninvasive imaging reagents for the determination of CO in living systems.

In recent years, several analytical technologies have been developed to

determination of CO in the chemical system, such as gas chromatography, [4] chromogenic detection, [5-7] and electrochemical assays. [8] However, most of these methods are effective for extracellular CO, while are not capable of precisely tracking real-time CO in vivo in a noninvasive manner. Compared with the traditional analytical technologies, fluorescence detection using fluorescent probes is more attractive due to its superiorities of convenience, high sensitivity, and real-time and nondestructive detection. [9-13] Up to now, several fluorescent probes have been developed and applied for cell-imaging of CO. [14-20] These reported fluorescent probes with absorption and emission in the blue–green light range have good performance at the cellular level. However, the in vivo applications are quite limited due to their poor capacity of resisting disturbance. One of the major obstacles encountered with fluorescence imaging of CO in vivo is the strong intrinsic autofluorescence background from living tissues, which significantly compromises the accuracy of measurement under physiological conditions. [21, 22] Near-infrared (NIR) fluorescent probes with long wavelength absorbance and emission (650–900 nm) are of considerable practical advantages due to decreased interference from background autofluorescence, minimum photo-damage to biological samples, high tissue depth penetration in the living systems. [23-29] Therefore, development of new NIR fluorescent probes of CO with improved properties and reliable signal in living cells is highly desired.

Herein, we developed a light-up NIR fluorescent probe system (probe 1 as shown in scheme 1) for colorimetric and fluorescent detection of CO, in which the chromophore DCPO is utilized as a NIR fluorescence reporter and an allyl carbonate unit is utilized as the CO-active trigger. DCPO are widely used in fluorescence imaging because of its NIR fluorescence and excellent light stability. [30, 31] The strategy of this probe relies on the in situ conversion of  $\text{Pd}^{2+}$  to  $\text{Pd}^0$  by CO and the well-known  $\text{Pd}^0$ -mediated Tsuji–Trost reaction to remove the allyl carbonate group. [32-34] The near infrared fluorescence Off-On switch is triggered by transformation of allyl carbonate unit to phenol by the interaction with CO, which results in the phenoxide anion formation ( $\text{DPCO}^-$ ). The probe system possesses several striking

merits as follows: firstly, it exhibits near-zero background fluorescence but shows a rapid, colorimetric, and remarkable NIR fluorescent turn-on response for CO, which allows a convenient visual and sensitive fluorescent detection for CO; secondly, it can be conveniently used to image both in vivo and in situ tracking of CO.

## 2. Experimental section

### 2.1. Materials and Instrumentation

All solvents and reagents used were analytical reagent and were used without further purification unless specified. [Ru(CO)<sub>3</sub>Cl-(glycinate)] (CORM-3) is a commercially available water-soluble CO-releasing molecule and can be used in the study as a CO source. Silica gel (200–300 mesh) bought from Qingdao Ocean Chemicals was used for column chromatography. Nitric oxide (NO) came from the aqueous solution of sodium nitroferricyanide dihydrate (CAS: 1313755-38-9). <sup>1</sup>H NMR and <sup>13</sup>C NMR spectra were recorded on a Bruker 600 MHz spectrometer using TMS as the internal standard. UV-vis spectra were recorded on a UV-2450 UV/Vis spectrophotometer (Shimadzu, Japan). Fluorescence spectra were measured with a fluorolog 3-TSCPC spectrophotometer (Horiba Jobin Yvon Inc.). All measurements were prepared in DMSO/PBS buffer solution (v:v=1:1, pH 7.4) and allowed to equilibrate at room temperature for 40 min before spectral measurements.

### 2.2. Compound synthesis and characterization

2-(2-(4-Hydroxystyryl)-4H-chromen-4-ylidene) malononitrile (DCPO) was synthesized according to the procedure published in literatures as shown in Scheme 2. [35, 36]

Synthesis of the Probe 1. To a solution of DCPO (312 mg, 1.0 mmol) in dry CH<sub>2</sub>Cl<sub>2</sub> (10 mL) was added Et<sub>3</sub>N (0.5 mL) under N<sub>2</sub> atmosphere. After stirring for 10 min, the resulting red solution was cooled in an ice-bath, and then allyl chloroformate (1.04 g, 4 mmol) was slowly added over 10 min. During this time, the reacted mixture changed to yellow and the solution was constantly stirred 14 hours at normal temperature. After filtration, the crude product was precipitated out from the filtrate under reduced pressure. The target product was afforded when the crude product was further purified by column chromatography (dichloromethane/ethyl acetate = 10:1,

v/v) as yellow solid (192.7 mg, 48.6%). m.p.168.3–170.1°C.  $^1\text{H}$  NMR (600 MHz, DMSO- $d_6$ )  $\delta$  (ppm): 8.75–8.74 (d,  $J=6.0$  Hz, 1H), 8.01–7.99 (d,  $J=12.0$  Hz, 1H), 7.96–7.93 (t,  $J = 9.0$  Hz, 1H), 7.85–7.79 (m, 3H), 7.64–7.62 (t,  $J=6.0$  Hz, 1H), 7.53–7.37 (m, 3H), 7.06 (s, 1H), 6.05–5.98 (m, 1H), 5.44–5.41 (d,  $J=18.0$  Hz, 1H), 5.34–5.32 (d,  $J=12.0$  Hz, 1H), 4.77–4.75 (t,  $J=6.0$  Hz, 2H).  $^{13}\text{C}$  NMR (150 MHz, DMSO- $d_6$ )  $\delta$  (ppm): 190.79, 157.10, 155.51, 153.05, 152.29, 137.51, 134.75, 132.53, 131.28, 130.90, 129.09, 126.05, 125.84, 121.85, 121.73, 119.84, 119.09, 118.63, 115.58, 107.09, 69.43, 63.21. EI-MS calcd for  $\text{C}_{24}\text{H}_{16}\text{N}_2\text{O}_4$  396.4, found 397.3[M+H] $^+$ .

### 2.3. Cell culture experiments

Breast cancer cells (MCF-7) were purchased from ATCC and were cultured in Dulbecco's Modified Eagle's Medium (DMEM) supplemented with 10% Fetal Bovine Serum (FBS), 100  $\mu\text{g}/\text{mL}$  penicillin and 100  $\mu\text{g}/\text{mL}$  streptomycin in a 5%  $\text{CO}_2$ , water saturated incubator at 37°C, and then were seeded in a 24-well culture plate for one night before cell imaging experiments. In the experiment of cell imaging, living cells were incubated with probe 1 (5  $\mu\text{M}$ ) and a mixture of probe 1 (5  $\mu\text{M}$ ) +  $\text{PdCl}_2$  (10  $\mu\text{M}$ ) at 37 °C for 30 min, respectively. For imaging of exogenous CO, MCF-7 cells were pretreated with CO (40  $\mu\text{M}$ ) for 40 min at 37 °C and then were incubated with a mixture of probe 1 (5  $\mu\text{M}$ ) +  $\text{PdCl}_2$  (10  $\mu\text{M}$ ) for 40 min at 37 °C. The imaging of CO was then carried out upon excitation at 400 nm, emission window of red channel and 20 $\times$  objective lens.

The in vitro cytotoxicity of the probe system was studied with Alamar blue assay. MCF-7 cells were seeded in 48-well plates at a density of  $1 \times 10^4$  cells per well. After 24 h attachment, variant concentrations of probe 1 and  $\text{PdCl}_2$  were added and incubated with the cells for another 24 h. Afterwards, the medium was removed and each well was washed with PBS for three times. 250  $\mu\text{L}$  Alamar blue solution was added to incubate with cells. 4h later, 200  $\mu\text{L}$  of this solution was pipetted from each well and transferred into a 96-well plate for measurement. The absorbance was read at 570 nm (excitation)/600 nm (emission) using an automated microplate spectrophotometer. The untreated cells were used as control and determined as 100% viability. The blank Alamar blue without incubation with cells were taken as blank

and used to calibrate the absorbance of each sample. The relative cell viability (%) could be calculated by the ratio of the calibrated absorbance of a sample to the calibrated absorbance of control group. Viable cells were stained green, while dead cells were stained red.

### 3. Results and discussion

#### 3.1. Colorimetric and Fluorescent Detection of CO

The absorption and fluorescence properties of the probe system (5  $\mu\text{M}$  probe 1 + 10  $\mu\text{M}$  PdCl<sub>2</sub>) were determined in PBS (pH =7.4) solution containing 50% of DMSO. As shown in Fig. 1A, the probe system has a main absorption peaks at around 375 nm and the solution of probe system shows light yellow. When the probe system was treated with CO for 40 min, a new absorption peaks appeared at 575 nm with a decrease of peak at 375 nm. The maximum absorption peak shifted from 375 nm to 575 nm. Along with increasing of CO concentration, the absorption titration curves of the probe system increased gradually at 575 nm and the solution of the probe system shows dark brown indicating the capacity of the probe system for colorimetric detection of CO. As shown in Fig.1B, there was a good linearity between the absorption intensity ( $A_{575}$ ) and concentration of CORM-3 ranging from 0 to 30  $\mu\text{M}$ :  $y=0.015+0.007\times[\text{CO}]$  ( $R^2=0.9906$ ).

To further identify the performance of the probe system, the emission spectra of the probe was measured by fluorescence titration experiment. As shown in Fig. 2A, the probe system showed almost no fluorescence emission upon excitation ( $\lambda_{\text{ex}}$ ) at 565 nm. Addition of CO resulted in an obvious increase at 685 nm. With increasing concentrations of CORM-3, the fluorescence titration spectrum showed a gradual enhancement. As shown in Fig. 2B, there was a good linearity between the fluorescence intensity at 685 nm and the concentration of CO ranging from 0 to 30 $\mu\text{M}$  (Fig. 2B):  $y=3737.7+1202.7\times[\text{CO}]$  ( $R^2=0.9980$ ). The detection limit of CO was calculated from the equation  $\text{DL}=3\sigma/S$ , where  $\sigma$  is the standard deviation of a blank measurement and S is the slope between intensity versus sample concentration. The detection limit of the probe system was calculated to be  $5.7\times 10^{-8}$  M. As shown in Fig. 3A, upon addition of 40  $\mu\text{M}$  of CORM-3, the probe system showed significant

time-dependent fluorescent changes in the fluorescence spectra. Remarkably, the fluorescence intensity of the probe solution at 685 nm reached nearly a maximum value within 40 min as shown in Fig.3B. The time-dependent fluorescent change measurements showed the response time of the probe system toward CO was 40 min (Fig. 3).

### 3.2. CO selective and competitive experiment

The selectivity of the probe system was examined towards CO, various anions and amino acids including  $F^-$ ,  $Cl^-$ ,  $Br^-$ ,  $I^-$ ,  $SO_4^{2-}$ ,  $HPO_4^{2-}$ ,  $HCO_3^-$ , Gly, Glu, Trp, Lys, Cys, GSH,  $HS^-$ ,  $ClO^-$ ,  $H_2O_2$ ,  $NO_2^-$ ,  $S_2O_3^{2-}$ ,  $N_2H_4$  and NO. As a result, only CO induced an obvious turn-on fluorescence changes at 685 nm. There was little fluorescence intensity increase when the probe system treated with other analytes (Fig. 4A). These results clearly indicate that this probe system is highly selective for CO. Besides, probe system had a good anti-interference for CO when mixing with others in competitive experiment (Fig. 4B). These results indicated that the probe system has reasonable selectivity to identify CO in a complex environment.

### 3.3. Fluorescence bio-imaging and cytotoxicity assay

On the basis of the excellent performances shown above, we investigated the potential applications of the probe system for imaging of CO in living cells. As shown in Fig. 5, when MCF-7 cells were incubated with probe 1 (5  $\mu$ M) or the probe system (5  $\mu$ M probe 1 + 10  $\mu$ M  $PdCl_2$ ) for 40 min, no fluorescence was observed (Fig.5b and Fig.5c). However, when the cell culture was pre-incubated the probe system, then incubated with CORM-3, intracellular red fluorescence was observed clearly (Fig.5d), indicating the probe system is indeed an effective probe candidate for monitoring intracellular CO changes in living cells.

To evaluate the cytotoxicity of the probe system, MCF-7 cells were incubated with various concentrations of probe 1 and  $PdCl_2$  for 24 h. The cell viabilities were evaluated via live/dead staining and Alamar blue assay. As the live/dead staining displayed, nearly all of the cells were stained green (live cells) at different probe system concentrations (Fig.6a and 6b). As shown in Fig. 6c, even when the concentration of the probe system was increased to as high as 15  $\mu$ M for probe 1 and

30  $\mu\text{M}$  for  $\text{PdCl}_2$ , stained green fluorescence (live cells) can be still observed. However, most of the cells were showed red fluorescence (dead cells) when treated with a high concentration of the probe system including 20  $\mu\text{M}$  probe 1 and 40  $\mu\text{M}$   $\text{PdCl}_2$  (Fig. 6d). The results of MTT assays also indicate that cell viability was over 85% when it is used below 15  $\mu\text{M}$  probe 1 and 30  $\mu\text{M}$   $\text{PdCl}_2$  (Fig. 7). Therefore, these results clearly indicate that the probe system possess low cytotoxicity to living cells.

### 3. Conclusion

In summary, a novel NIR fluorescent probe system of CO was prepared. It showed admirable detection performances for CO with apparent colorimetric response, evident fluorescence turn-on phenomenon, an ideal testing limit as low as 0.57  $\mu\text{M}$ , and low cytotoxicity to living cells. More importantly, this probe system has been successfully applied to detect CO in living cells by laser confocal microscopy imaging. Because of these excellent properties, this probe system possessed great potential for practical applications in detection of CO in living systems.

### Acknowledgements

This work was supported by Guangxi Key Laboratory of Electrochemical and Magnetochemical Functional Materials (EMFM20181107), Policy Guidance Program (Research Cooperation) Prospective Joint Research Project (BY2016076-02), National Major Scientific Instruments and Equipment Development Projects (2014YQ060773) and the Project Funded by the Priority Academic Program Development of Jiangsu Higher Education Institutions (1107047002).

### References and notes

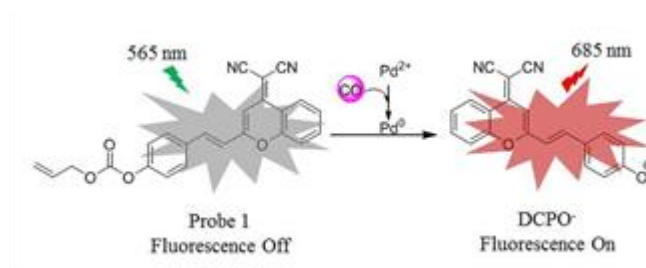
- [1] L. Wu, R. Wang, Carbon monoxide: endogenous production, physiological functions, and pharmacological applications, *Pharmacol. Rev.* 57(2005), 585–630.
- [2] A. Verma, D.J. Hirsch, C. E. Glatt, G.V. Ronnett, S. H. Snyder, Carbon monoxide: a putative neural messenger, *Science* 259(1993), 381–384.
- [3] R. Motterlini, L. E. Otterbein, The therapeutic potential of carbon monoxide, *Nat. Rev. Drug Discov.* 9(2010), 728–743.
- [4] G.S. Marks, H.J. Vreman, B.E. Mclaughlin, J.F. Brien, K. Nakatsu, Measurement of endogenous carbon monoxide formation in biological systems, *Antioxid. Redox Signal.*

- 4(2002), 271–277.
- [5] D. Benito-Garagorri, M. Puchberger, K. Mereiter, K. Kirchner, Stereospecific and reversible CO binding at iron pincer complexes, *Angew. Chem. Int. Ed.* 47(2008), 9142–9145.
- [6] S. Heylen, J. A. Martens, Progress in the chromogenic detection of carbon monoxide, *Angew. Chem. Int. Ed.* 49(2010), 7629–7630.
- [7] M.E. Moragues, J. Esteban, J.V. Ros-Lis, R. Martínez-Máñez, M.D. Marcos, M. Martínez, J. Soto, F. Sancenon, Sensitive and selective chromogenic sensing of carbon monoxide via reversible axial CO coordination in binuclear rhodium complexes, *J. Am. Chem. Soc.* 133(2011), 15762–15772.
- [8] Y. Lee, J. Kim, Simultaneous electrochemical detection of nitric oxide and carbon monoxide generated from mouse kidney organ tissues, *Anal. Chem.* 79(2007), 7669–7675.
- [9] X. Wu, L. Li, W. Shi, Q. Gong, X. Li, H. Ma, Sensitive and selective ratiometric fluorescence probes for detection of intracellular endogenous monoamine oxidase A, *Anal. Chem.* 88(2016), 1440–1446.
- [10] Z.-R. Dai, G.-B. Ge, L. Feng, J. Ning, L.-H. Hu, Q. Jin, D.-D. Wang, X. Lv, T.-Y. Dou, J.-N. Cui, L. Yang, A highly selective ratiometric two-photon fluorescent probe for human cytochrome P450 1A, *J. Am. Chem. Soc.* 137(2015), 14488–14495.
- [11] Z. Mao, H. Jiang, Z. Li, C. Zhong, W. Zhang, Z. Liu, An N-nitrosation reactivity-based two-photon fluorescent probe for the specific in situ detection of nitric oxide, *Chem. Sci.* 8(2017), 4533–4538.
- [12] A.T. Aron, M.O. Loehr, J. Bogen, C.J. Chang, An endoperoxide reactivity-based FRET probe for ratiometric fluorescence imaging of labile iron pools in living cells, *J. Am. Chem. Soc.* 138(2016), 14338–14346.
- [13] Y.-R. Wang, L. Feng, L. Xu, Y. Li, D.-D. Wang, J. Hou, K. Zhou, Q. Jin, G.-B. Ge, J.-N. Cui, L. Yang, A rapid-response fluorescent probe for the sensitive and selective detection of human albumin in plasma and cell culture supernatants, *Chem. Commun.* 52(2016), 6064–6067.
- [14] J. Wang, J. Karpus, B.S. Zhao, Z. Luo, P.R. Chen, C. He, A selective fluorescent probe for carbon monoxide imaging in living cells, *Angew. Chem. Int. Ed.*, 51(2012), 9652–9656.
- [15] B.W. Michel, A.R. Lippert, C.J. Chang, A reaction-based fluorescent probe for selective

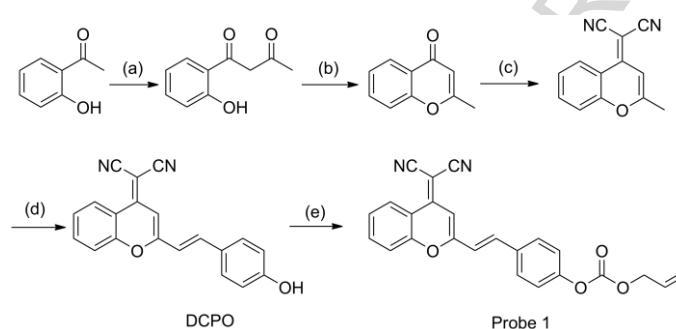
- imaging of carbon monoxide in living cells using a palladium-mediated carbonylation, *J. Am. Chem. Soc.* 134(2012), 15668–15671.
- [16] K. Zheng, W. Lin, L. Tan, H. Chen, H. Cui, A unique carbazole–coumarin fused two-photon platform: development of a robust two-photon fluorescent probe for imaging carbon monoxide in living tissues, *Chem. Sci.* 5(2014), 3439–3448.
- [17] S. Pal, M. Mukherjee, B. Sen, S. K. Mandal, S. Lohar, P. Chattopadhyay, K. Dhara, A new fluorogenic probe for the selective detection of carbon monoxide in aqueous medium based on Pd (0) mediated reaction, *Chem. Commun.* 51(2015), 4410–4413.
- [18] Z. Xu, J. Yan, J. Li, P. Yao, J. Tan, L. Zhang, A colorimetric and fluorescent turn-on probe for carbon monoxide and imaging in living cells, *Tetrahedron Lett.* 57(2016), 2927–2930.
- [19] Y. Li, X. Wang, J. Yang, X. Xie, M. Li, J. Niu, L. Tong, B. Tang, Fluorescent probe based on azobenzene-cyclopalladium for the selective imaging of endogenous carbon monoxide under hypoxia conditions, *Anal. Chem.* 88(2016), 11154–11159.
- [20] W. Feng, D. Liu, S. Feng, G. Feng, Readily available fluorescent probe for carbon monoxide imaging in living cells, *Anal. Chem.* 88(2016), 10648–10653.
- [21] Z. Guo, W. Zhu, H. Tian, Dicyanomethylene-4H-pyran chromophores for OLED emitters, logic gates and optical chemosensors, *Chem. Commun.* 48(2012), 6073–6084.
- [22] W. Zhu, X. Huang, Z. Guo, X. Wu, H. Yu, H. Tian, A novel NIR fluorescent turn-on sensor for the detection of pyrophosphate anion in complete water system, *Chem. Commun.* 48(2012), 1784–1786.
- [23] L.K. Truman, S. Comby, T. Gunnlaugsson, Real-time tracking and in vivo visualization of  $\beta$ -galactosidase activity in colorectal tumor with a ratiometric near-infrared fluorescent probe, *Angew. Chem. Int. Ed.* 51(2012), 9624–962.
- [24] B.K. McMahon, T. Gunnlaugsson, Selective detection of the reduced form of glutathione (GSH) over the Oxidized (GSSG) form using a combination of glutathione reductase and a Tb(III)-cyclen maleimide based lanthanide luminescent ‘Switch On’ assay, *J. Am. Chem. Soc.* 134(2012), 10725–10728.
- [25] L.Y. Niu, Y.S. Guan, Y.Z. Chen, L.Z. Wu, C.H. Tung, Q.Z. Yang, BODIPY-based ratiometric fluorescent sensor for highly selective detection of glutathione over cysteine and homocysteine, *J. Am. Chem. Soc.* 134(2012), 18928–18931.

- [26] L. Yuan, W. Lin, K. Zheng, L. He, W. Huang, Far-red to near infrared analyte-responsive fluorescent probes based on organic fluorophore platforms for fluorescence imaging, *Chem. Soc. Rev.* 42(2013), 622–661.
- [27] X. Wang, Z. Guo, S. Zhu, H. Tian, W.H. Zhu, A naked-eye and ratiometric near-infrared probe for palladium via modulation of a  $\pi$ -conjugated system of cyanines, *Chem. Commun.* 50(2014), 13525–13528.
- [28] S. Lim, K. Hong, D.I. Kim, H. Kwon, H. Kim, Tunable heptamethine-azo dye conjugate as an NIR fluorescent probe for the selective detection of mitochondrial glutathione over cysteine and homocysteine, *J. Am. Chem. Soc.* 136(2014), 7018–7025.
- [29] K. Gu, Y. Xu, H. Li, Z. Guo, S. Zhu, S. Zhu, P. Shi, T. D. James, H. Tian, W.-H. Zhu, Real-time tracking and in vivo visualization of  $\beta$ -galactosidase activity in colorectal tumor with a ratiometric near-infrared fluorescent probe, *J. Am. Chem. Soc.* 138(2016), 5334–5340.
- [30] X. Zhang, L. Zhang, Y. Liu, B. Bao, Y. Zang, J. Li, W. Lu, A near-infrared fluorescent probe for rapid detection of hydrogen peroxide in living cells, *Tetrahedron* 71(2015), 4842–4845.
- [31] B. Bao, M. Liu, Y. Liu, X. Zhang, Y. Zang, J. Li, W. Lu, NIR absorbing DICPO derivatives applied to wide range of pH and detection of glutathione in tumor, *Tetrahedron* 71(2015), 7865–7868.
- [32] F. Song, A.L. Garner, K. Koide, A highly sensitive fluorescent sensor for palladium based on the allylic oxidative insertion mechanism, *J. Am. Chem. Soc.* 129(2007), 12354–12355.
- [33] A.L. Garner, F. Song, K. Koide, Enhancement of a catalysis-based fluorometric detection method for palladium through rational fine-tuning of the palladium species, *J. Am. Chem. Soc.* 131(2009), 5163–5171.
- [34] S. Feng, D. Liu, W. Feng, G. Feng, Allyl fluorescein ethers as promising fluorescent probes for carbon monoxide imaging in living cells, *Anal. Chem.* 89(2017), 3754–3760.
- [35] J. Fan, W. Sun, Z. Wang, X. Peng, Y. Li, J. Cao, A fluorescent probe for site I binding and sensitive discrimination of HSA from BSA, *Chem. Commun.* 50(2014), 9573–9576.
- [36] K. Gu, Y. Xu, H. Li, Z. Guo, S. Zhu, S. Zhu, P. Shi, T. D. James, H. Tian, W.-H. Zhu. Real-time tracking and in vivo visualization of  $\beta$ -galactosidase activity in colorectal tumor with a ratiometric near-infrared fluorescent probe, *J. Am. Chem. Soc.* 138(2016), 5334–5340.

## Schemes and figures



Scheme 1. The structure and reaction mechanism of the probe 1



Scheme 2. Synthesis of probe 1. (a)  $\text{Na}$ ,  $\text{CH}_3\text{COOC}_2\text{H}_5$ , 51%; (b)  $\text{H}_2\text{SO}_4$ ,  $\text{CH}_3\text{COOH}$ , 62%; (c) malononitrile,  $\text{AcOH}$ ,  $\text{H}_2\text{SO}_4$ , 14 h, 36.4%; (d) malononitrile,  $\text{CH}_3\text{COOCH}_3$ , 25%; (e)  $\text{Et}_3\text{N}$ , allyl chloroformate,  $\text{CH}_2\text{Cl}_2$ , 48.6%.

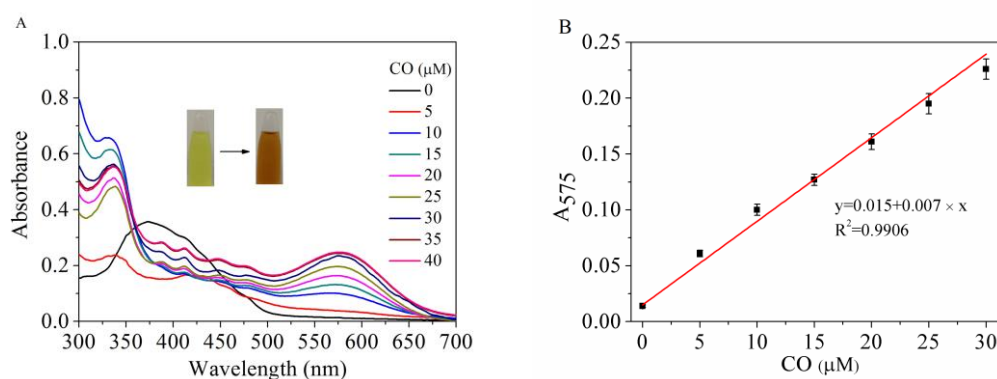


Fig.1. (A) Absorption spectra of probe (5  $\mu\text{M}$  probe 1 + 10  $\mu\text{M}$   $\text{PdCl}_2$ ) in the presence of different concentration of CORM-3 in PBS buffer (10 mM, pH 7.4, with 50% DMSO, v/v) at 37  $^\circ\text{C}$ , (B) a linear correlation between absorption intensity ( $A_{575}$ ) and concentration of CORM-3.

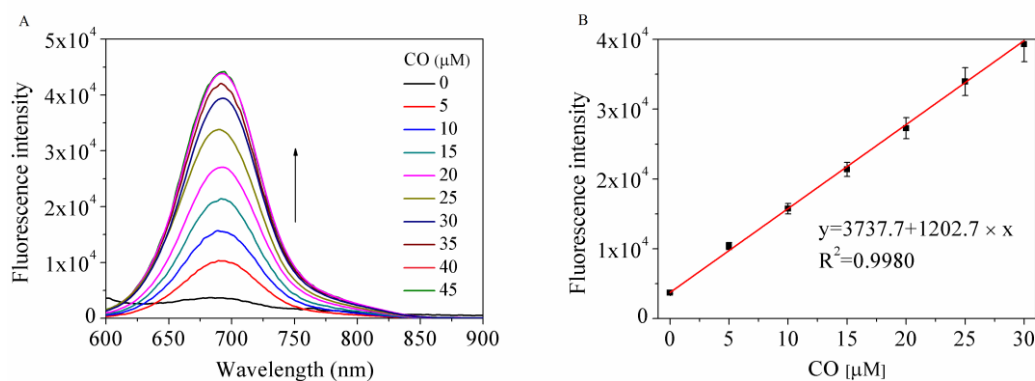


Fig.2. (A) Emission spectra ( $\lambda_{\text{ex}}=565$  nm) of probe (5  $\mu\text{M}$  probe 1 + 10  $\mu\text{M}$  PdCl<sub>2</sub>) in the presence of different concentration of CORM-3 in PBS buffer (10 mM, pH 7.4, with 50% DMSO, v/v) at 37 °C; (B) a linear correlation between emission intensity and concentration of CORM-3 at 685 nm.

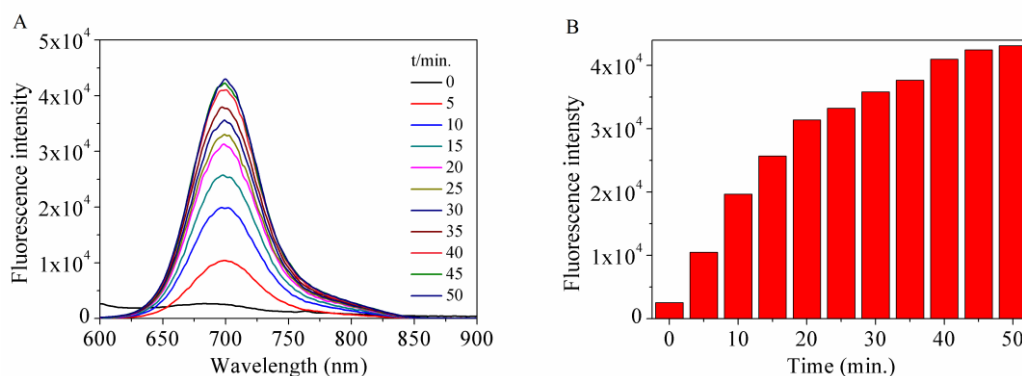


Fig.3. (A) Fluorescence spectra ( $\lambda_{\text{ex}}=565$  nm) changes of the probe (5  $\mu\text{M}$  probe 1 + 10  $\mu\text{M}$  PdCl<sub>2</sub>) upon addition of CORM-3 (40  $\mu\text{M}$ ) in PBS buffer (10 mM, pH 7.4, with 50% DMSO, v/v) at 37 °C. (B) Fluorescent intensity changes at 685 nm as a function of time.

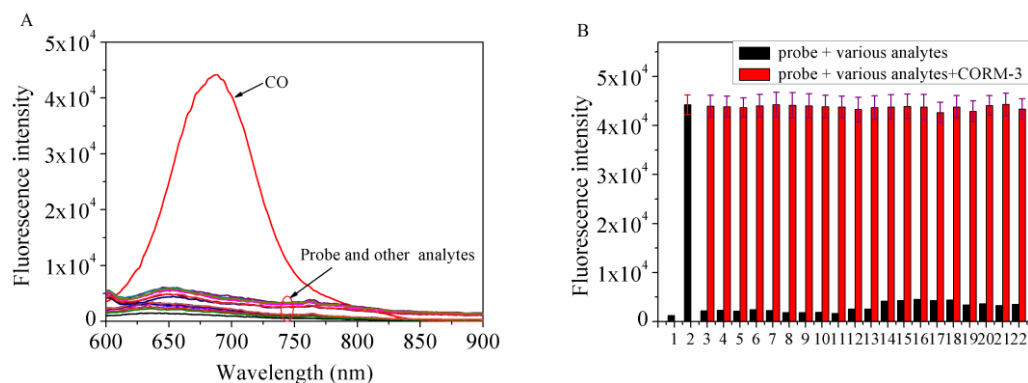


Fig.4. (A) Fluorescence response of the probe system (5  $\mu\text{M}$  probe 1 + 10  $\mu\text{M}$  PdCl<sub>2</sub>) to various analytes (40  $\mu\text{M}$ ) in PBS buffer (10 mM, pH 7.4, with 50% DMSO, v/v).

(B) Fluorescence intensity at 685 nm of the probe system (5  $\mu\text{M}$  probe 1 + 10  $\mu\text{M}$   $\text{PdCl}_2$ ) in the presence of various analytes (40  $\mu\text{M}$ ). Black bars represent the addition of 40  $\mu\text{M}$  of the appropriate analytes to the probe system (5  $\mu\text{M}$  probe 1 + 10  $\mu\text{M}$   $\text{PdCl}_2$ ). Red bars represent the addition of the probe system (5  $\mu\text{M}$  probe 1 + 10  $\mu\text{M}$   $\text{PdCl}_2$ ) to the mixture solution of 40  $\mu\text{M}$  the appropriate analytes and 40  $\mu\text{M}$  CORM-3. Analytes: (1) None, (2) CO, (3)  $\text{F}^-$ , (4)  $\text{Cl}^-$ , (5)  $\text{Br}^-$ , (6)  $\text{I}^-$ , (7)  $\text{SO}_4^{2-}$ , (8)  $\text{HPO}_4^{2-}$ , (9)  $\text{HCO}_3^-$ , (10) Gly, (11) Glu, (12) Trp, (13) Lys, (14) Cys, (15) GSH, (16)  $\text{HS}^-$ , (17)  $\text{ClO}^-$ , (18)  $\text{H}_2\text{O}_2$ , (19)  $\text{NO}_2^-$ , (20)  $\text{S}_2\text{O}_3^{2-}$ , (21)  $\text{N}_2\text{H}_4$  and (22) NO.

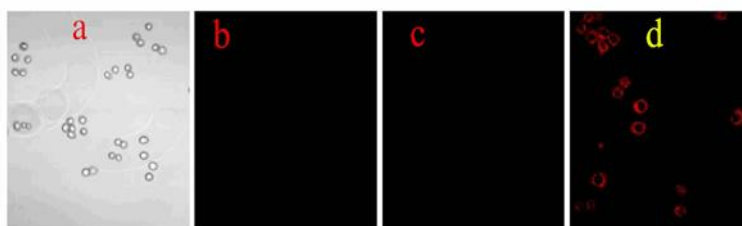


Fig.5. Confocal microscope images of MCF-7 cells. (a) bright field image of untreated cells; (b) cells treated with probe 1 (5 $\mu\text{M}$ ) for 40 min; (c) cells treated with 5  $\mu\text{M}$  probe 1 and 10  $\mu\text{M}$   $\text{PdCl}_2$  for 40 min; (d) cells treated with probe 1 (5  $\mu\text{M}$ ) +  $\text{PdCl}_2$  (10  $\mu\text{M}$ ) and subsequent treatment with CORM-3 (10  $\mu\text{M}$ ) for 40 min. (b) (c) and (d) images of cells upon excitation at 400 nm, emission window of red channel and 20 $\times$  objective lens.

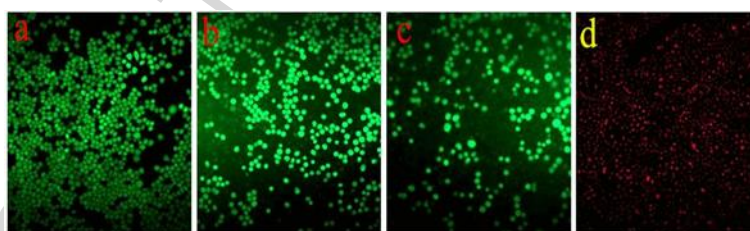


Fig.6. Cytotoxicity of probe 1. Fluorescence images of MCF-7 cells incubated with variant concentrations of probe 1 and  $\text{PdCl}_2$  for 24 h: (a) 5  $\mu\text{M}$  probe 1 + 10  $\mu\text{M}$   $\text{PdCl}_2$ , (b) 10  $\mu\text{M}$  probe 1 + 20  $\mu\text{M}$   $\text{PdCl}_2$ , (c) 15  $\mu\text{M}$  probe 1 + 30  $\mu\text{M}$   $\text{PdCl}_2$  and (d) 20  $\mu\text{M}$  probe 1 + 40  $\mu\text{M}$   $\text{PdCl}_2$ . The live cells were stained green, and the red indicates the dead cells.

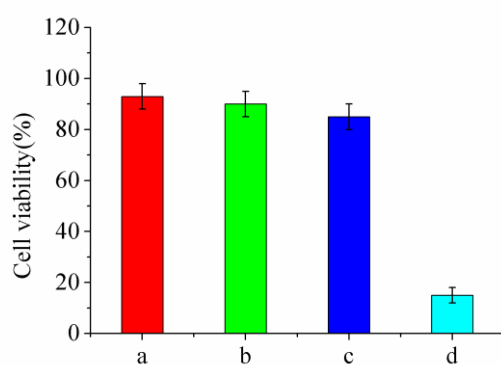
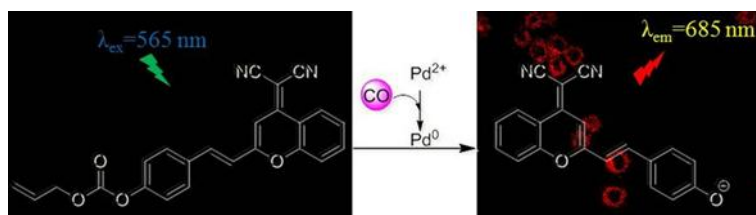


Fig.7. Cell viability of MCF-7 cells after incubated with variant concentrations of probe 1 and PdCl<sub>2</sub> for 24 h. (a) 5  $\mu$ M probe 1 + 10  $\mu$ M PdCl<sub>2</sub>, (b) 10  $\mu$ M probe 1 + 20  $\mu$ M PdCl<sub>2</sub>, (c) 15  $\mu$ M probe 1 + 30  $\mu$ M PdCl<sub>2</sub> and (d) 20  $\mu$ M probe 1 + 40  $\mu$ M PdCl<sub>2</sub>.

## Graphical Abstract



A near-infrared (NIR) and colorimetric fluorescent probe system was developed via a Pd<sup>0</sup>-mediated Tsuji–Trost reaction, which showed colorimetric and excellent turn-on responses for CO.

---

**Highlights**

- Near-infrared (NIR) fluorescence emission.
- Distinct colorimetric and excellent turn-on responses to CO.
- Low cytotoxicity and bio-imaging in living cells.

ACCEPTED MANUSCRIPT